

High Efficiency of a Folate Receptor Alpha Targeted Photodynamic Therapy on Epithelial Ovarian Cancer Patient-Derived Tumor Organoids Resistant to Parpi

Léa Boidin ^{1#}, Lucie Thorel ^{2,3#}, Camille Trioen ^{1*}, Roman Vion ⁴, Hippolyte Paysant ², Martha Baydoun ¹, Olivier Morales ^{1,5}, Romane Florent ⁶, Louis-Bastien Weiswald ^{2,3,6}, Laurent Poulain ^{2,3,6}, Nadira Delhem ¹

¹Univ. Lille, Inserm, CHU Lille U1189 - ONCO-THAI - Assisted Laser Therapy and Immunotherapy for Oncology, Lille, France.

²Univ. Caen Normandie, INSERM U1086 ANTICIPE (Interdisciplinary Research Unit for Cancers Prevention and Treatment), BioTICLA Laboratory (Precision Medicine for Ovarian Cancers), Caen, France.

³UNICANCER, Comprehensive Cancer Center François Baclesse, Caen, France.

⁴Department of Medical Oncology, Centre Henri Becquerel, Rouen, France.

⁵Univ. Lille, CNRS, Inserm, CHU Lille, UMR9020-U1277 - CANTHER – Cancer Heterogeneity Plasticity and Resistance to Therapies, F-59000 Lille, France.

⁶Université de Caen Normandie, Services Unit PLATON, ORGAPRED Core Facility, Caen, France.

***Corresponding Author:** Camille Trioen, Univ. Lille, Inserm, CHU Lille U1189 - ONCO-THAI - Assisted Laser Therapy and Immunotherapy for Oncology, Lille, France.

Received Date: November 08, 2024 | **Accepted Date:** December 04, 2024 | **Published Date:** December 31, 2024

Citation: Léa Boidin, Lucie Thorel, Camille Trioen, Olivier Morales, Nadira Delhem, et al, (2024), High Efficiency of a Folate Receptor Alpha Targeted Photodynamic Therapy on Epithelial Ovarian Cancer Patient-Derived Tumor Organoids Resistant to Parpi, *International Journal of Clinical Case Reports and Reviews*, 21(1); DOI:10.31579/2690-4861/604

Copyright: © 2024, Camille Trioen. This is an open-access article distributed under the terms of the Creative Commons Attribution License, which permits unrestricted use, distribution, and reproduction in any medium, provided the original author and source are credited.

Abstract:

Epithelial Ovarian Cancer (EOC) is the seventh cause of cancer-related deaths in women. The inhibition of poly-ADP-ribose polymerase (PARP) by PARP inhibitors (PARPi), such as Olaparib, has considerably improved the outcome of patients with homologous recombination deficiency (HRD) status. However, the major toxicity of PARPi combined with the emergence of resistance has led to the development of innovative strategies that can be used in combination or alone in order to optimize treatment and improve patient prognosis. The aim of this study was to use EOC cell line and Patient-Derived Tumor Organoids (PDTO) to provide key information on the potential of an innovative treatment based on folate receptor alpha (FR α)-targeted PDT combined or not to PARPi, in the context of intrinsic or acquired drug resistance. Interestingly, we showed for the first time that organoids derived from EOC cell line and Patient-Derived Tumor Organoids (PDTO) resistant to PARPi exhibited an excellent sensitivity to FR α -targeted PDT. Furthermore, PDT alone is sufficient to induce PDTOs death and prior treatment with PARPi does not improve therapeutic efficacy. These results provide new perspectives about the potential of PDT to overcome resistance to conventional treatment which open new therapeutic option for EOC.

Key words: photodynamic therapy; PARP inhibitors; patient-derived tumor organoids; ovarian cancer; folate receptor alpha

Introduction

Ovarian carcinoma (OC) is a highly frequent condition associated with a poor prognosis, with around 200,000 deaths worldwide by 2022 [1]. Among OC, Epithelial Ovarian Cancer (EOC) is the most frequent subtype and the deadliest, representing 90% of OC cases and the most common EOC histological subtypes (70%) is the high grade serous

ovarian carcinoma (HGSOC) [2]. Due to the lack of symptoms of EOC in early stages, 80% of patients are diagnosed with an advanced disease (stage III or IV according to the FIGO classification) [3]. In these advanced stages, widespread intra-abdominal disease with peritoneal

metastases is often present and is characterized as peritoneal carcinosis [4].

The advent of poly-ADP-ribose polymerase inhibitors (PARPi) (e.g., Olaparib, Niraparib, Rucaparib) has dramatically changed the prognosis of patient with peritoneal carcinosis from epithelial origin. Around 50% of HGSOC present a homologous recombination (HR) deficiency (HRD) status, including 15%-20% of germline BRCA1/2 mutations [5]. PARP inhibition prevents the repair of DNA single-strand breaks (SSBs) by transforming them into double-strand breaks (DSBs) that cannot be repaired in an HRD context, thus leading to synthetic lethality. Somatic BRCA1/2 mutations, hypermethylation of the BRCA1 promoter and deficiency in other proteins involved in the HR pathways contribute to the remainder of HRD. Although these PARPi have provided clinical benefit among patients with germline and/or tumor BRCA mutation and/or HRD tumors [6], they are not devoid of toxicities and poorly tolerated. Furthermore, although some patients exhibit intrinsic resistance to PARPi, various acquired resistance mechanisms (e.g., BRCA reversion mutation, restoration of HR repair function, replication fork stabilization, epigenetic changes) can lead to disease progression during PARPi therapies [5,7–9]. Therefore, combinatorial therapeutics strategies are a cornerstone in cancer therapeutics that may be leveraged to (i) enable dose reductions of PARPi while maximizing anti-cancer effects

(ii) resensitize patients who developed PARPi resistance (iii) switch from an HRP to an HRD status.

PDT has emerged as a new innovative treatment methodology in cancer [10]. This minimally invasive treatment, involves the light-activation of a photosensitive drug (PS) causing a photochemical reaction that releases reactive oxygen species (ROS) thus leading to direct tumor cell death and the modulation biological processes such as the establishment of an anti-tumor immune response thanks to its immunogenic cell death properties [11]. More interestingly, the use of PDT for EOC has already been evaluated in phase I and II clinical trials, but severe morbidity (e.g. digestive perforation, capillary leak syndrome and pleural effusion) and no significant objective complete response were observed, mainly due to the lack of tumor specificity for PS uptake. Based on these studies, precise targeting of peritoneal residual cancer cells by PS is required to enable intraperitoneal PDT for EOC. The cell surface protein, folate receptor alpha (FR α) which is overexpressed in 75% of women suffering from EOC [12–15] in contrast to its highly restricted expression in normal tissues represents an interesting biomolecular target with clinical promising prospect in resistant patients.

We have developed and patented a FR α targeted PS (i.e., Folic Acid conjugated to pyropheophorbide-a (Pyro- a) via a polyethylene glycol (PEG) type spacer, named Pyro-PEG-FA, (patent WO/2019/016397)) for PDT treatment of Peritoneal metastases of OC to specifically target

peritoneal residual ovarian cancer cell overexpressing FR α . In previous studies, we have shown that this Pyro-PEG-FA was capable to induce direct human ovarian tumor cells death and enhance the activation of the immune system [16]. In vivo, in a humanized mice model of peritoneal ovarian cancer, this targeted PDT exhibited a decrease of the tumor growth and the induction of an anti-tumor immune response was reflected by an increase in the percentage of innate and adaptative immune cells [17].

Preclinical models of cancer are essential to develop effective treatments, and clinical-relevant models that can capture the inter-patient heterogeneity are even more needed in the era of personalized medicine. Although 2D cell lines are widely used as pre-clinical models and are suitable for numerous functional testing they only poorly reflect the patient tumor heterogeneity [18]. Furthermore, some resistance to PDT has already been observed in 3D tumor models compared to 2D ones [19]. For this reason, the evaluation of a new therapies on relevant model like patient-derived tumor Organoids (PDTO) should not be underestimated to evaluate the potential patient's response.

PDTO can form self-organized 3D micro-tumors that reflect the initial tumor in terms of histological and molecular characteristics [20]. PDTO can efficiently be derived from ovarian tumor [21–23] and a study comparing an ovarian PDTO model with other preclinical models showed that PDTO recapitulated the patient's response while being more relevant than 2D cell lines and faster and more easily cultured than PDX [24]. PDTOs thus represent models close to the clinic that can be used for functional testing and for research purposes.

Head and neck PDTO have been used for testing in vitro EGFR-targeted PDT [25] and 3D model derived from OC cell line to evaluate benzoporphyrine derivative PDT combined to chemotherapy [26], but to our knowledge, no study to date has assessed the value of FR α -targeted PDT alone on ovarian PDTO and in combination with PARPi. This ambitious interdisciplinary study aims to evaluate first, the efficiency of a new innovative FR α - targeted PDT on different preclinical OC models and secondly to evaluate its efficiency in combination with PARPi in PDTO models resistant to PARPi and derived from OC.

Materials and Methods

Photosensitizer. The present study use a PS patented by our research unit (patent number WO/2019/016397). Its chemical structure is shown in Figure 1 and is based on folic acid conjugated to pyropheophorbide-a (Pyro) via a polyethylene glycol (PEG) type spacer. The synthesis and the photophysical properties, has already been described in the patent quoted above and its biological effect in previous in vitro and in vivo studies [16,17].

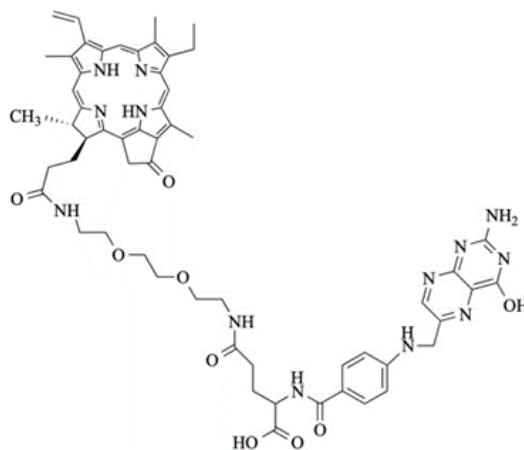


Figure 1: Structure of the Pyro-PEG-FA: folic acid conjugated to pyropheophorbide-a via a polyethylene glycol type spacer.

Ovarian Cancer Cell lines

Cell line culture. OC cell lines (OVCAR3 and SKOV3) were ordered from the American Type Culture Collection (ATCC, Manassas, Virginia, USA). SKOV3 cells were cultured in 50% DMEM medium (4.5 g/L D-glucose, L-glutamine, Gibco, Thermo Fisher Scientific, Waltham, MA, USA) and 50% F-12 (Ham's F-12 Nutrient Mix, Gibco, Thermo Fisher Scientific, Waltham, MA, USA) and OVCAR3 cells were cultured in RPMI-1640 medium (Gibco, Thermo Fisher Scientific, Waltham, MA, USA). The mediums were supplemented with 10% heat inactivated fetal calf serum (Gibco, Thermo Fisher Scientific, Waltham, MA, USA) and with 100 units/mL penicillin and 100 µg/mL streptomycin (Gibco, Thermo Fisher Scientific, Waltham, MA, USA). Cells were maintained in an incubator at 37°C, 5% CO₂, and 95% humidity.

Evaluation of the Pyro-PEG-FA incorporation. Adherent cells were cultured on glass coverslips in 12-well plates (Corning, Somerville, MA, USA). 24 h after plating, 9 µM of Pyro-PEG-FA were added to the wells during 24 h. The cell monolayers were washed with PBS (Gibco, Thermo Fisher Scientific, Waltham, MA, USA) and fixed with paraformaldehyde (PFA 4%; Alfa Aesar). After 3 washes, cells were incubated for 1 h at RT in PBS containing gelatin (1.2%), glycine (0.2 M) and tween-20 (0.05%) (Sigma-Aldrich, St Louis, MO, USA) for blocking. After washing, the cells were incubated for 1 h with the primary FR α polyclonal antibody (Rabbit/IgG) (Invitrogen, Thermo Fisher Scientific, Waltham, MA, USA), diluted (1:400) in PBS overnight at 4°C and after washing, incubated with the secondary antibody Alexa Fluor 555 (Invitrogen, Thermo Fisher Scientific, Waltham, MA, USA) (1:300) diluted in PBS for 1 h at room temperature (RT). After washing, the nuclei were counterstained with DAPI (Thermo Fisher Scientific, Waltham, MA, USA). Coverslips were mounted in Glycergel (Agilent Dako, C056330-2, Santa Clara, California, USA, USA) and observed using a LSM 710 inverted confocal microscope (Leica, Wetzlar, Germany). Photographic images were resized, organized, and labeled using Fiji-ImageJ software V2.3.0/1.53q.

Cell lines response to PDT. OVCAR3 cell line (10 000 cells) and SKOV3 cell line (5.000 cells) were seeded in a white clear bottom 96-well plates (Corning, Somerville, MA, USA). After 24 h, the medium was replaced by a fresh one containing Pyro-PEG-FA at different concentrations from 0 to 4.5 µM (0, 0.14, 0.28, 0.56, 1.12, 2.25 and 4.5 µM). 24 h later, the medium containing PS was changed and replaced by the usual medium of the cell type after two washing steps with PBS. A homogeneous

illumination (1 mW/cm²) was then performed at 1.8 J/cm² with a specific 672 nm laser-based device developed by our research unit [38]. All the experiments were performed in dark conditions. Cancer cell lines viability after PDT was assessed 24 h after the treatment by CellTiterGlo assay according to the manufacturer instruction (CellTiterGlo®, Promega, Madison, WI, USA). The luminescence (RLU) was quantified using a luminometer ClarioStar Plus (BMG Labtech, Champsigny sur Marne, France) driven by MARS™ Software v2.06. Viability values were normalized to non-treated control and treatment sensitivity was expressed as the average of three independent replicates expressed in percentage of Normalized Viability.

3D cultures derived from cell lines

3D cultures derived from the OVCAR3 cell line establishment. 3D cultures were derived from the OVCAR3 cell line previously described. 2000 isolated cells were seeded in domes of 20 µL containing 2:3 growth factor-reduced matrigel (Corning® 356231) and 1:3 organoid-specific medium. Specific medium contained 50% Advanced DMEM basal medium (Gibco, Thermo Fischer) and 50% prepared medium containing: 10% HA-E-Spondin1-Fc 293 T conditioned medium, 50% L-WRN conditioned medium, N-Acetyl-L-cysteine (1.25 mM), Supplement B27 100X (Thermo Fischer), recombinant mouse EGF (50 ng/ml) (Thermo Fischer), recombinant human FGF-10 (20 ng/ml) (Peprotech), recombinant human FGF-Basic (1 ng/ml), A-83-01 (500nM), Y-27632 dihydrochloride (10 µM) (Stemcell), SB202190 (1 µM) (Gibco, ThermoFischer), Nicotinamide (10 mM) (Sigma-Aldrich), Prostaglandin E2 (1 µM) (SigmaAldrich). 3D cultures were maintained in culture for 15 days at 37°C under 5% CO₂ before being transferred to 96-well plates for PDT treatment.

FR α expression. 2000 OVCAR3 cells were seeded in Matrigel domes affixed on a coverslip in a 24-well plate (Corning, Somerville, MA, USA) containing 1 Matrigel dome/well. After 20 days of culture, the medium was removed and incubated with 4% PFA for 20 min at RT then washed with PBS. 3D cultures were permeabilized with a 0.2% saponin solution diluted in PBS (Sigma-Aldrich) for 20 min at RT. The non-specific sites were then saturated with a mixture of 0.2% saponin and 3% BSA (Sigma-Aldrich) for 20 min at RT. Anti-FR α primary antibody (Polyclonal antibody, Rabbit IgG, Invitrogen) was incubated in the same solution at 4°C overnight.

After 3 washes with PBS, the secondary antibody (Alexa Fluor 488 goat anti-rabbit IgG, Invitrogen) was added for 1 h 30 at RT in the dark. Slides were mounted on coverslips using 15 μ L of mounting liquid (Vectashiel®, Vector Laboratories) per slide on SuperFROST slides (CML) and observed using a LSM 710 inverted confocal microscope (Leica, Wetzlar, Germany). Photographic images were resized, organized, and labeled using Fiji- ImageJ software V2.3.0/1.53q.

3D cultures derived from the OVCAR3 cell line response to PDT.

Organoids were seeded in a white clear bottom 96-well plates (Corning, Somerville, MA, USA). After 24 h, the medium was replaced by a fresh one containing Pyro-PEG-FA at 9 μ M. 24 h later, the medium containing Pyro-PEG-FA was changed and replaced by the usual medium after two washing steps with PBS. A homogeneous illumination (1 mW/cm²) was then performed at 3.6 J/cm² with the same laser-based device as previously described. All the experiments were performed in dark conditions. Organoids viability after PDT was assessed 24 h after the treatment by 3D CellTiterGlo assay according to the manufacturer instruction (CellTiterGlo®, Promega, Madison, WI, USA). The luminescence (RLU) was quantified using a luminometer ClarioStar Plus (BMG Labtech, Champigny sur Marne, France) driven by MARS™ Software v2.06. Treatment sensitivity was expressed as the average of three independent replicates expressed in percentage in RLU.

Patient-derived tumor organoids (PDTO)

Ethical considerations and regulatory aspects. Fresh tumoral tissue from EOC were collected from patients treated at the Comprehensive Cancer Center Francois Baclesse (Unicancer Center, Normandy) by the Biological Resources Center ‘OvaRessources’ (NF-S 96900 quality management, AFNOR No. 2016: 72860.5). The biological collection was declared to the French Ministry of Education, Health and Research (No. DC 2010- 1243). Informed consent form was signed by the patients and was obtained under the agreement of the ethical committee “North-West III” (CPP).

PDTO characteristics. OV-150_A and OV-174_T were derived from patients diagnosed with a HGSOE at a FIGO stage IV with no BRCA mutation. OV-174_T was derived from a tumor tissue extracted from the ovary and OV- 150_A was derived from an ascites sample.

PDTO culture. PDTO were obtained from tumor dissociated cells or filtered ascites as previously described [27]. Cells were collected in organoid basal medium (OBM: Advanced DMEM (Fisher Scientific), 10 UI/mL penicillin, 10 μ g/mL streptomycin, 1% GlutaMAX-1 (Fisher Scientific)) and pelleted (2 000 rpm for 5 min). Cells were then resuspended in organoid culture medium (OBM containing B27 (Fisher Scientific, 200 μ L/mL), N- Acetyl-L-cysteine (Sigma, 1.25mM), EGF (Miltenyi, 50ng/mL), FGF-10 (Peprotech, 20ng/mL), FGF-basic (Miltenyi, 1ng/mL), A-83-01 (Peprotech, 500nM), Y27632 (Selleckchem, 10 μ M), SB202190 (Peprotech, 1 μ M), Nicotinamide (Sigma, 10mM), PGE2 (Sigma, 1 μ M), Primocin (InvivoGen, 100 μ g/mL), Cultrex HA-R-Spondin-1- Fc 293T (AmsBio, 10% V/V) and Cultrex L-WRN (AMS Bio, 50% V/V)). Then, 50 μ L drops of 1:1 growth factor-reduced BME2 (Bio Techne)/cell suspension containing 10 000 cell per drops were allowed to solidify on prewarmed 24-well suspension culture plates. After polymerization (37°C, 5% CO₂, 15 min), each drop was immersed with 500 μ L of organoid culture medium. Medium was renewed twice a week and PDTO were passaged every 2-3 weeks: PDTO were collected with cold OBM supplemented with 1% BSA, centrifuged

at 200g for 2 min and incubated with TrypLE Express (Gibco, ThermoFischer) for up to 10 min at 37°C. After dissociation, cells were centrifuged at 430g for 5 min, resuspended in organoid culture medium and counted. Then, 50 μ L drops of BME2-cell suspension (10 000 cell per drops) were placed in prewarmed 24-well plates. Upon completed gelation, organoid culture medium was added to each well. Plates were then transferred to a humidified 37°C/5% CO₂ incubator. PDTO lines were authenticated by comparison of their short tandem repeat (STR) profiles with that of sample of origin (Microsynth).

FR α expression. Tumor tissue and PDTO were fixed in 3% PFA overnight. After embedding PDTO in 2% agarose, tissue and PDTO were dehydrated, paraffin embedded, and sectioned before standard HES staining. Automated immunohistochemistry using a Ventana Discovery XT autostainer (Roche) was performed on 4 μ m- thick paraffin sections. Slides were deparaffinized with EZPrep buffer and epitopes were unmasked by 15 min of high-temperature treatment in CC1 EDTA buffer. Sections were incubated for 40 min at 37°C with an anti- FR α (ab221543, Abcam, 1/1500). Secondary antibody (Omnimap Rabbit HRP; Ventana Medical System Inc., Tucson, AZ, USA) was incubated for 16 min at room temperature. Immunodetection performed without the primary antibody was used as control. After washes, the staining was performed with DAB (3, 3'- diaminobenzidine) and sections were counterstained with hematoxylin using Ventana reagents according to the manufacturer's protocol. Stained slides were then digitized using an Aperio ScanScope slide scanner (Aperio Technologies).

PDTO response to Olaparib. Olaparib (Medchemexpress) was diluted in DMSO and stored as a 50 mM stock solution at -80°C. Response of PDTO to treatment was assessed as previously described [28]. When PDTO reached the size of 75-150 μ m in diameter, they were collected with cold OBM supplemented with 1% BSA and centrifugated at 200 g for 2 min. Next, the pellet was resuspended in organoid treatment medium (organoid culture medium lacking primocin, Y-27632 and N-acetylcysteine) and counted. PDTO were resuspended in 2% BME2/organoid treatment medium and 200 PDTO per well were seeded in 100 μ L volume in a previously coated (1:1 treatment medium/BME2) white clear bottom 96-well plates (Greiner). Thirty minutes later, PDTO were exposed to Olaparib and plates were transferred to a humidified 37°C/5% CO₂ incubator. During the treatment, PDTO were monitored using IncuCyte S3 ZOOM (Sartorius). One week later, ATP levels were measured by CellTiter-Glo 3D assay and luminescence was quantified using GloMax Plate Reader (Promega). Viability values were normalized to control and treatment sensitivity was expressed as the average of two independent replicates. To determine status of resistance to Olaparib, results were compared to a collection of other HGSOE PDTO, one reference PDTO was displayed.

Evaluation of the Pyro-PEG-FA incorporation. PDTO were cultured in 6-well plates (Corning, Somerville, MA, USA) and incubated with 9 μ M of Pyro-PEG-FA during 24 h. Then, the PDTO were washed with PBS and the nuclei were counterstained with Hoescht (Thermo Fisher Scientific, Waltham, MA, USA). PDTO were then directly observed using a SP8 confocal microscope Gx25, W0.0.95 (Leica, Wetzlar, Germany). Photographic images were resized, organized, and labeled using Fiji-ImageJ software V2.3.0/1.53q.

PDTO response to combination therapy. PDTO were seeded and exposed to Olaparib for one week as described above. During the treatment, plates were kept on a humidified 37°C, 5% CO₂ incubator. One

week later, medium was removed and PDTO were washed with PBS. PDTO were then exposed to a solution of Pyro- PEG-FA at different concentrations (0, 1.12, 2.25, 3.5 and 4.5 μM). 24 h later, the medium containing Pyro- PEG-FA was changed and replaced by the usual medium after two washing steps. A homogeneous illumination (1 mW/cm^2) was then performed at 1.8 J/cm^2 with the same laser-based device previously described. 24 h after the illumination, the viability was evaluated using CellTiterGlo 3D assay as described above. Viability values were normalized to control and treatment sensitivity was expressed as the average of two independent replicates.

Statistical Analysis

All results were expressed as the means and standard deviations or standard error of the mean of triplicates of at least three independent experiments. All data were analyzed using the statistical package GraphPad Prism for Windows 3.0.1 (GraphPad, San Diego, CA, USA). The normality of the distributions was assessed using the Shapiro–Wilk test. All quoted p-values are two-sided, with $p \leq 0.05$ (*), $p \leq 0.01$ (**), $p \leq 0.001$ (***), and $p \leq 0.0001$ (****) being considered statistically significant for the first and highly significant for the other.

Results

PDT is effective on FR α -expressing ovarian cancer cell lines

The fluorescence properties of the Pyro-PEG-FA were used to assess its uptake by confocal microscopy while the FR α expression by the OC cell lines was confirmed by immunofluorescence (Figure 2). Visual analysis of FR α labeling (in green) confirmed FR α membrane expression by OVCAR3 and SKOV3 cell lines (Figure 2A.1). Regarding the Pyro-PEG-FA uptake (in red), we noticed an incorporation after 24 h of incubation into both the cell lines (Figure 2A.1), which was higher for the OVCAR3 cells compared to SKOV3 cells (Figure 2A.2) thus confirming the capacity of the FR α positive cells to internalize the Pyro-PEG-FA.

After validating the Pyro-PEG-FA incorporation into OC cells, we evaluated the efficacy of PDT. In this regard, cells were incubated with various concentrations of PS for 24 h and then illuminated at 1.8 J/cm^2 . Viability was assessed 24 h post-treatment (Figure 2B). We observed that OC cells were sensitive to PDT through a dose response curve. Moreover, we noticed that OVCAR3 cells were more sensitive to the treatment than SKOV3 cells (EC_{50} OVCAR3 = 0.174 μM vs EC_{50} SKOV3 = 0.476 μM). Finally, we demonstrated that none of Pyro-PEG-FA concentration tested was cytotoxic to the cells in dark condition.

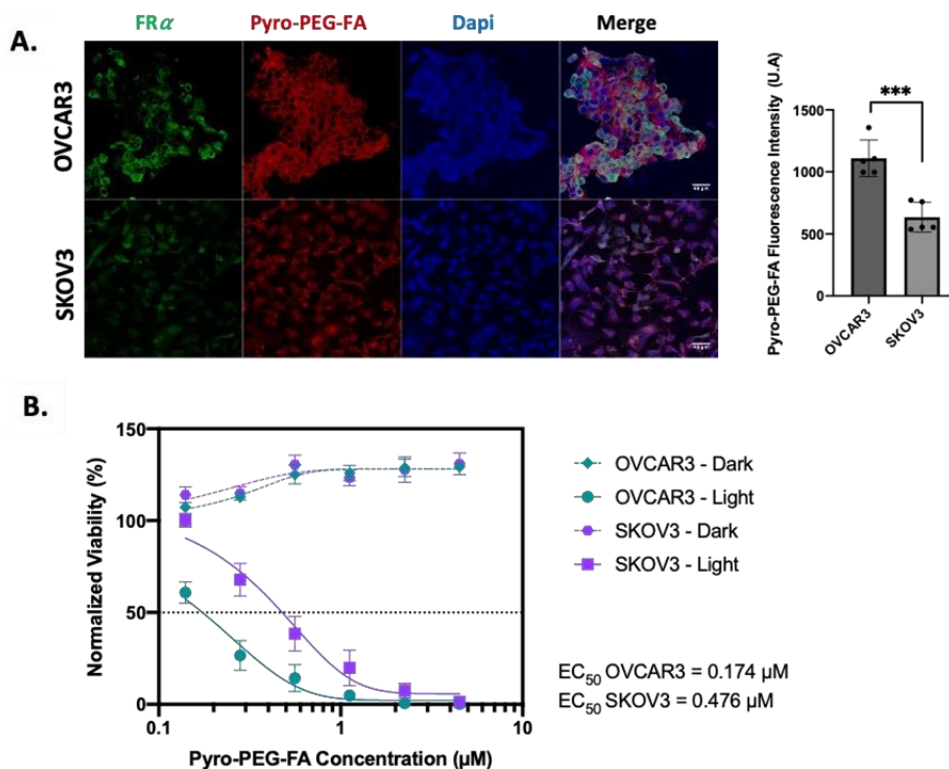


Figure 2: Sensitivity of Ovarian Cancer cell lines to FR α targeted PDT. (A.) Images of Confocal microscopy for FR α expression and Pyro- PEG-FA accumulation in OVCAR3, SKOV3 cell lines cultured with 9 μM of PS for 24 h and observed at Gx40 (left) and semi- quantification of PS fluorescence intensity expressed in U.A (right). (B) Percentage of Normalized Viability for OVCAR3, SKOV3 cell lines 24 h post-PDT treatment. Cells were incubated with increasing concentrations of Pyro-PEG-FA (0.14, 0.28, 0.56, 1.12, 2.25 and 4.5 μM) for 24 h. Illumination was performed with laser set at 672 nm coupled to a specific device delivering 1 mW/cm^2 and with a light dose of 1.8 J/cm^2 . Results are represented as mean \pm SEM of 3 independent experiments, expressed in percentage (%) compared to Non- Treated (NT) cells condition. (n=5).

PDT is effective on 3D cultures derived from ovarian cancer cell lines

Next, we wanted to evaluate the PDT potential in more complex 3D model derived from cell lines. First, the FR α expression in 3D cultures derived from the OVCAR3 cell line was evaluated by

immunofluorescence (Figure 3A). Fluorescence (in green) reflecting FR α expression confirmed the expression of the receptor by the established 3D cultures after 15 days of culture.

To evaluate the efficacy of PDT, 3D cultures were incubated with 9 μM of Pyro-PEG-FA for 24 h. Based on previous studies [16,17], the organoids were then irradiated at 3.6 J/cm² with an irradiance of 1 mW/cm². Cell-derived 3D cultures structures were evaluated by IHC at 48h and 72h (Figure 3B) and viability was assessed 1h, 24h, 48h and 72h post-treatment (Figure 3C).

Regarding the morphological aspect of the 3D cultures in PDT condition, the structure looked strongly altered by the treatment 48 h and 72 h post PDT. This is even more interesting, as none of these changes were observed under the other control conditions (Figure 3 B). These

observations were confirmed with the viability test as we observed a strong and significant decrease of the viability in the PDT condition from 1 h post PDT ($p=0.0049$) (Figure 3C). Furthermore, 24 h post-illumination, this decrease was even more significant ($p=0.0006$) and sustained throughout the assay (until 72 h post-PDT). Concerning the control condition, we found a slight but significant decrease of the viability in the Pyro-PEG-FA and illumination condition 24 h post treatment ($p=0.0158$ and $p=0.0220$ respectively) but this observation was not found anymore 72 h post treatment and remained largely lower than the PDT-condition.

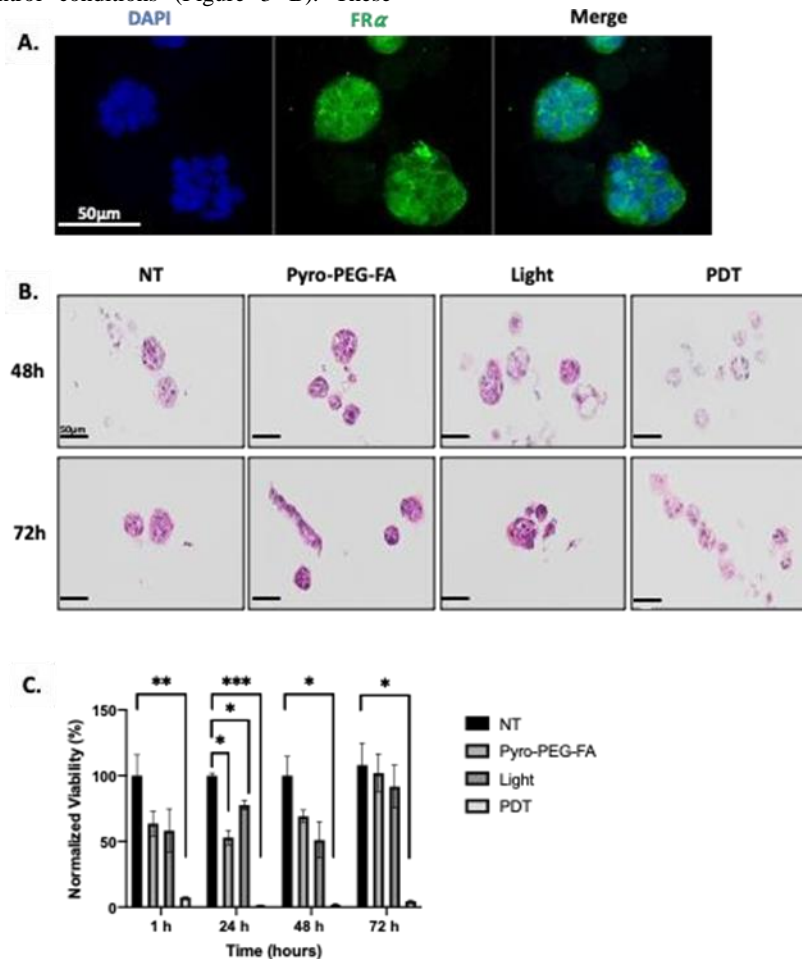


Figure 3: Sensitivity of organoids derived from ovarian cancer cell line to Fra targeted PDT. (A) Images of Confocal microscopy-based FR α expression in organoids derived from OVCAR3 and observed at Gx40 (scale bar = 50 μM). (B) IHC analysis of organoids 48 h and 72 h after PDT. (C) Percentage of normalized viability of the organoids derived from OVCAR3 cell line after PDT treatment. Organoids were treated with 9 μM of PS for 24 h. Illumination was performed with laser set at 672 nm combined to a device delivering 1 mW/cm² and with a light dose of 3.6 J/cm². Results are represented as mean \pm SEM of 3 independent experiments, expressed in percentage (%) compared to Non-Treated (NT) condition. NT: non-treated; Pyro-PEG-FA: photosensitizer only; Light: illumination only; PDT: illumination in the presence of the Pyro-PEG-FA.

Patient-derived tumor organoids response to PARPi and Fra targeted PDT

Selection of two samples of PDTO resistant to PARPi and eligible to Fra targeted PDT

In order to have a better in vitro model that faithfully represent the patient tumor heterogeneity, we investigated if PDT could open a new therapeutic option for patient resistant to PARPi in ovarian PDTO lines. Firstly, we performed a selection based on two criteria: (i) resistance to PARPi and (ii) expression of the FR α . Based on our first selection criteria, different

PDTOs were treated with increasing concentrations of Olaparib and their viability was measured 7 days after treatment (Figure 4A). We intended to use 2 models of PARPi-resistant PDTOs with different degrees of resistance. OV-174_T (derived from a tumor sample) and OV-150_A (derived from an ascites sample) displayed both resistant profile after olaparib treatment in comparison with a reference PDTO with an EC₅₀ of 48.7 μM , 47.1 μM and 11.6 μM respectively (Figure 4A right).

Based on the second selection criteria and to assess the efficacy of PDT on PDTOs, we confirmed the expression of the target protein FR α on those two PDTOs by IHC (Figure 4B). We performed an analysis on

original tissue and on the resulting PDTOs. We noticed an expression of FR α on original tissue and on PDTO (in brown). Even if the FR α

expression is slightly lower in PDTO than in the original tissue it remains important and should be sufficient to perform PDT.

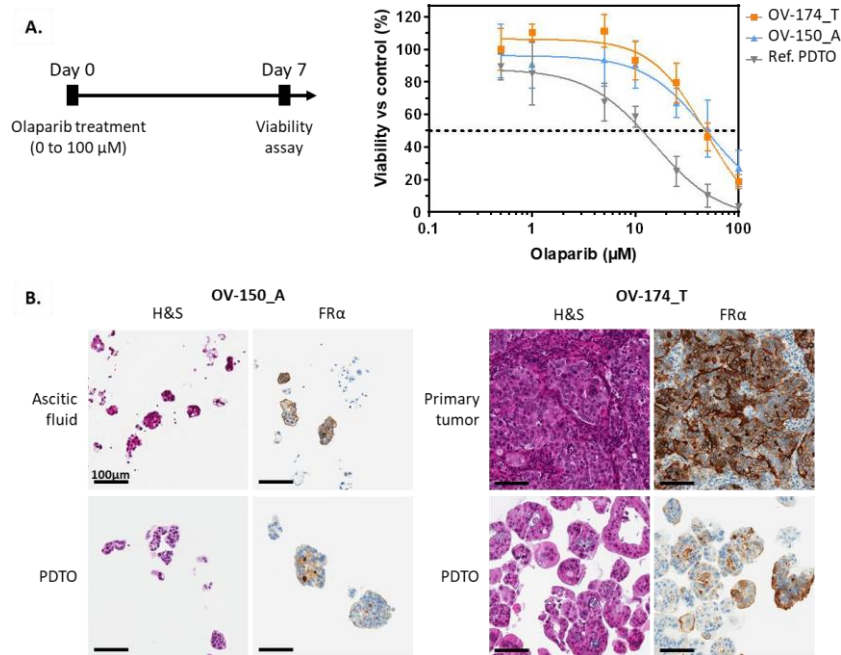


Figure 4: Selection of PDTO resistant to PARPi and eligible to FR α targeted PDT. (A) Percentage of normalized viability of the OV- 150_A, OV-174_T and reference PDTO after 7 days of olaparib treatment. Results are represented as mean \pm SD of at least 2 independent experiments. (B) HES and FR α staining of the primary tumor sample and the paired patient-derived tumor organoids for each model selected. Scale = 100 μ m.

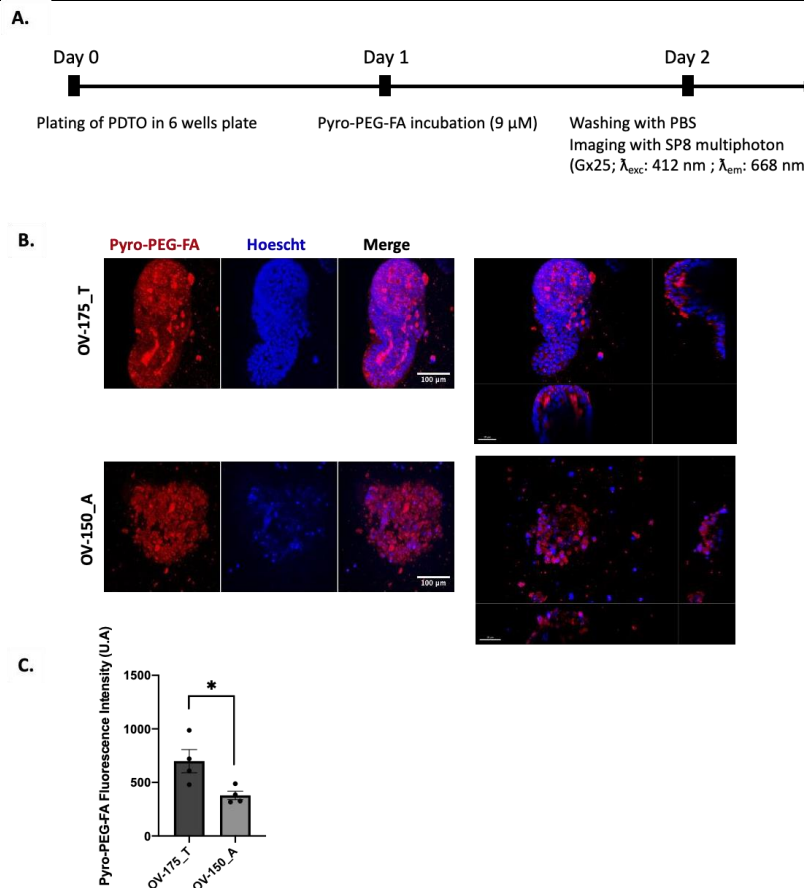


Figure 5: Evaluation of PS uptake within PDTO. (A) Timeline of the treatment (B) Images of Confocal microscopy-based Pyro-PEG-FA uptake with living PDTOs cultured with 9 μ M of Pyro-PEG-FA for 24 h and observed at Gx25 (Confocal SP8 multiphoton). Scale bar = 100 μ m (left) and 50 μ m (right). (C) Semi-quantification of the Pyro-PEG-FA uptake. Histograms are represented as mean \pm SEM of 4 independents experiments.

After confirming the FR α expression, we assessed Pyro-PEG-FA incorporation by living PDTO with imaging thanks to the fluorescence properties of the PS (Figure 5A). We observed a strong red signal reflecting the incorporation of the PS with the two models of PDTO (Figure 5B). The semi-quantification highlighted a greater incorporation for OV-174_T ($p=0.0319$) (Figure 5C). These results suggest that these PDTOs, resistant to PARPi and expressing FR α , might be sensitive to PDT.

PDTO response to the PARPi-PDT combination treatment

Then, we evaluated the sensitivity of the PDTOs to FR α targeted PDT alone or in combination with Olaparib. Given the high sensitivity of the organoids derived from OVCAR3 cell line to the light dose of 3.6 J/cm² we reduced the light dose to 1.8 J/cm² (the same dose as the in vitro model).

For the PDTOs treated with PDT alone, we observed a dose-dependent decrease in cell viability for both types of PDTOs (Figure 6A). We noticed a greater sensitivity of OV-150_A with a decrease of 90 % in viability at a concentration of 3.5 μ M, whereas for OV-174_T, we observed a decrease of 20 % at the same concentration.

When PDTOs were treated with PARPi for 7 days and then incubated with the photosensitive drug in dark condition (Figure 6B, PARPi + PS

only), we did not notice any effect of the Pyro-PEG-FA since the dose response curve observed was close to the one representing the sensitivity of PDTO to PARPi (Figure 3A). In fact, at the highest concentration of PARPi, the viability of OV-174_T remained at 30% and OV-150_A at 16% confirming the resistance of these models to PARPi. The same observation was noticed when PDTOs were treated with PARPi and illuminated without Pyro-PEG-FA. These results demonstrated that the photosensitive drug alone or the illumination alone do not impact the viability of the organoids when they are treated with PARPi.

Finally, we investigated the effect of the combination PARPi + PDT. PDTOs were first incubated one week with Olaparib before being treated with Pyro-PEG-FA and illuminated (Figure 6C). After bi-therapy treatment, we observed a decrease in PDTOs viability that was dose-dependent on the amount of Pyro-PEG-FA (Figure 6D). However, it appears that PDT alone is sufficient to induce PDTOs death. Indeed, at the highest concentrations of Pyro-PEG-FA (4.5 μ M in OV-174_T and 3.5 μ M in OV-150_A), we observed a decrease in viability that was not dependent on the concentration of Olaparib, resulting in the absence of a dose-response curve. These results tend to show that PDT alone is sufficient to induce PDTOs death and that prior treatment with PARPi does not improve therapeutic efficacy.

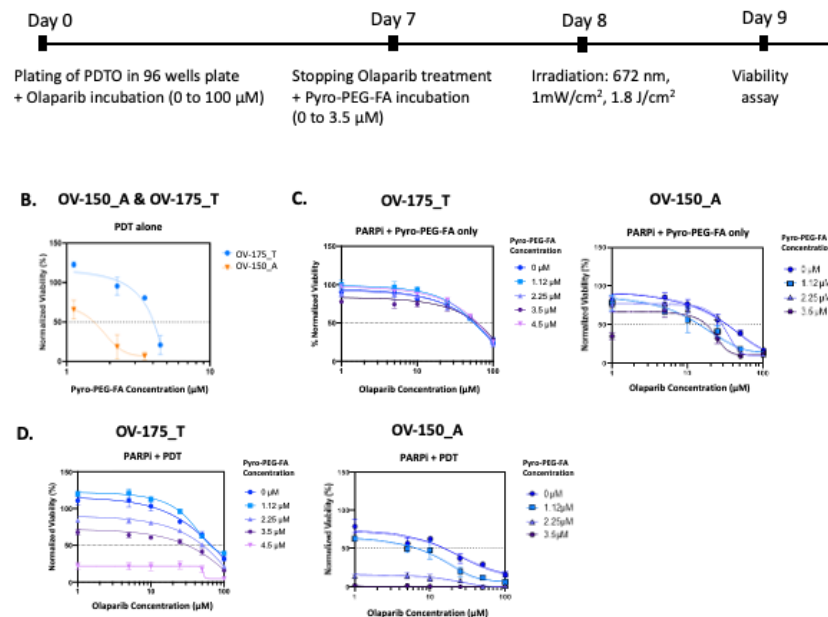


Figure 6: Efficacy of the therapeutic combination PARPi-PDT: (A) Timeline of the combination PARPi – PDT, (B) Percentage of normalized viability of the PDTO after PDT treatment only, (C) after PARPi-Pyro-PEG-FA only treatment, and after (D) the PARPi-PDT treatment. Results are represented as mean \pm SD of at least 2 independent experiments.

Discussion

EOC is one of the most challenging diseases in gynecological oncology, with 80% of advanced cases relapsing after initial therapies [29]. Improved first-line strategy are urgently needed to enhance patient prognosis. In this context, PARPi has emerged to treat ovarian cancers but also various malignancies (e.g., breast, pancreatic, prostate, fallopian and primary peritoneal cancers) [30]. Despite significant improvements in outcomes for patients with HRD thanks to PARPi [29], two major issues remain: (i) PARPi are not devoid of toxicities (ii) resistance to

PARPi has been described in both preclinical and clinical settings [5]. Therefore, strategies to reduce side effects associated with PARPi and/or overcome PARPi resistance through combinational therapeutic approaches are urgently needed.

In this context, PDT is an emerging treatment modality in oncology that could be relevant. We previously developed and patented a vectorized PS coupled to Folic Acid in order to target FR α which is overexpressed in 80% of EOC. The effectiveness and the immunogenic properties of this

PDT using this photosensitive drug has already been demonstrated in vitro et in vivo in our previous study [16,17].

Preclinical data have demonstrated powerful combination effects of PARPi with PDT [31–33] which could be beneficial for patient. Tanaka et al. were able to show in a gastric cell model that PDT treatment mediated by the photosensitizer talaporfin followed by 48h of exposure to Olaparib produced a synergistic response to the treatments. These results were then confirmed in a xenograft mouse model, with a reduction in tumor volume in the combination condition [32]. Another study in pancreatic cancer demonstrated the strong synergistic effect of PDT mediated by the second-generation photosensitizer chlorin e6 co-delivered with Olaparib in a cell culture model [31]. These last two studies were based on cell culture models, but other teams proposed to use more complex models and were able to test co-delivery of a photosensitizer with the PARPi talazoparib in an ovarian 3D culture model, demonstrating the efficacy of this combination [33]. With the aim of always working with more clinically relevant models, PDOs were also studied, with the study of EGFR- targeted photodynamic therapy in head and neck PDOs [34]. Nevertheless, to our knowledge, no study to date has assessed the value of FR α -targeted PDT in combination with PARPi in ovarian PDO models. Therefore, the present study aimed to evaluate for the first time the efficiency of this FR α targeted PDT on PDOs selected for their resistance to PARPi. The objectives were to assess the clinical potential of PDT alone for patient resistant to conventional treatments and to evaluate the clinical relevance of the combination of PDT to PARPi.

First, we established dose response curve in a 2D model of ovarian cancer. We observed that the OVCAR3 cell line was more sensitive to PDT than SKOV3 cell line likely due to higher FR α expression in OVCAR3. This difference in PDT sensitivity might also reflect differences in behavior of the primary tumor types from which the cell lines were derived. High-grade serous ovarian carcinoma (HGSOC), from which OVCAR3 is derived, presents at an advanced stage, grows rapidly and spread throughout the peritoneal cavity. In contrast, non- serous tumors (NS) from which SKOV3 is derived, commonly present an early stage and formed large tumor mass. Surprisingly, Amelia Hallas-Potts et al., found that NS cell lines migrated more rapidly than HGSOC and were more invasive which seems counter-intuitive to the clinic. Therefore, even if the conventional 2D cell culture has long been established and allows for a rapid and reliable growth of cancer cells, the major drawback of this model is its inability to reproduce the clinical cancer spectrum [35].

It is essential to develop new models that recapitulate the biological characteristics of tumors and their microenvironment. For this reason, PDOs can fill the gaps left by cell lines in the testing of new drugs, especially as EOC is a heterogeneous disease and accurate assessment of tumor heterogeneity is important for predicting drug resistance and seeking effective treatments [36]. We have therefore further complicated the 2D model by establishing organoids derived from OVCAR3 cell lines. We increased the light dose at 3.6 J/cm² and showed that these spheroids were very sensitive to PDT. This allowed us to demonstrate the efficacy of PDT in a more complex cellular model.

Nevertheless, PDOs offer a promising preclinical platform, enabling personalized medicine for EOC patient. PDOs closely recapitulate heterogeneity of the biological properties of the original tumor and can be used for drug screening and studying resistance mechanisms [37]. We and others have developed different models of ovarian cancer PDOs derived

from patients with different mutational profiles and responses to treatments [21–24], demonstrating the relevance of PDO as clinical avatars reflecting the real-life heterogeneity.

We selected two PDO models, OV-150_A and OV-174_T, derived from ovarian ascites and tumor tissue respectively, that both displayed a resistance to olaparib. Firstly, we ensured FR α expression within the original tumors and PDOs and showed that even lower expression levels in PDO compared to original tumor were sufficient for the Pyro-PEG-FA to target tumor cells and allow PDT efficacy, resulting in a dose dependent decrease in PDO viability. Next, we evaluated therapeutic combination of PDT and PARPi and the therapeutic combination did not show a synergistic effect between the two therapies, with the PDT efficacy dominating the whole, reflected in particular at the highest concentrations of Pyro-PEG-FA by the presence of a straight line rather than a dose-response curve. However, we demonstrated the efficacy of PDT in a complex patient- derived models that displayed resistance to PARPi suggesting that PDT could be a promising approach to target tumor cells resistant to conventional treatments.

Finally, we aware of the crucial importance of the tumor microenvironment (immune cells, blood vessels, etc.) in tumor growth and treatment response. As PDT is known to induce robust anti-tumor immune response, develop co-culture system in the presence of immune cells (dendritic cells [38], NK cells [39], macrophages [40] and lymphocytes [41]) to recapitulate inter-cell interactions and communication remains a key point to evaluate immunostimulating properties of PDT.

Conclusions

EOC has a poor prognostic and its management remains a challenge between disseminated malignancies and chemoresistance. In this context, the development of innovative therapeutics strategies as well as more pertinent in vitro models to test them is crucial. In this article we provide evidences of the efficiency of FR α based PDT on different models from immortalized ovarian cell lines to patient-derived tumor organoids. We particularly focused on models displaying a resistance to both carboplatin and PARPi and, even if no synergy was observed when PDT was combined to PARPi, we were able to report for the first time very promising results showing the efficacy of PDT in a context of global resistance to standard first-line chemotherapeutic regimen. PDT should thus open up new treatment prospects for EOC and in the long-term for other cancers overexpressing FR α .

References

1. Bray, F.; Laversanne, M.; Sung, H.; Ferlay, J.; Siegel, R.L.; et al. (2024). Global Cancer Statistics 2022: GLOBOCAN Estimates of Incidence and Mortality Worldwide for 36 Cancers in 185 Countries. *CA Cancer J Clin* 74, 229–263, doi:10.3322/caac.21834.
2. Gaona-Luviano, P.; Medina-Gaona, L.A.; Magaña-Pérez, K. (2020). Epidemiology of Ovarian Cancer. *Chin Clin Oncol* 9, 47, doi:10.21037/cco-20-34.
3. van Baal, J.O.A.M.; van Noorden, C.J.F.; Nieuwland, R.; Van de Vijver, K.K.; Sturk, A.; et al. (2018). Development of Peritoneal Carcinomatosis in Epithelial Ovarian Cancer: A Review. *J Histochem Cytochem* 66, 67–83, doi:10.1369/0022155417742897.

4. Berek, J.S.; Renz, M.; Kehoe, S.; Kumar, L.; Friedlander, M. (2021). Cancer of the Ovary, Fallopian Tube, and Peritoneum: 2021 Update. *Int J Gynaecol Obstet* 2021, 155, 61–85, doi:10.1002/ijgo.13878.
5. Chiappa, M.; Guffanti, F.; Bertoni, F.; Colombo, I.; Damia, G. (2021). Overcoming PARPi Resistance: Preclinical and Clinical Evidence in Ovarian Cancer. *Drug Resistance Updates* 55, 100744, doi:10.1016/j.drug.2021.100744.
6. O'Malley, D.M.; Krivak, T.C.; Kabil, N.; Munley, J.; Moore, K.N. (2023). PARP Inhibitors in Ovarian Cancer: A Review. *Target Oncol* 18, 471–503, doi:10.1007/s11523-023-00970-w.
7. Francica, P.; Rottenberg, S. (2018). Mechanisms of PARP Inhibitor Resistance in Cancer and Insights into the DNA Damage Response. *Genome Med* 2018, 10, 101, doi:10.1186/s13073-018-0612-8.
8. Hill, S.J.; Decker, B.; Roberts, E.A.; Horowitz, N.S.; Muto, M.G.; et al. (2018). Prediction of DNA Repair Inhibitor Response in Short-Term Patient-Derived Ovarian Cancer Organoids. *Cancer Discov* 8, 1404–1421, doi:10.1158/2159-8290.CD-18-0474.
9. Lord, C.J.; Ashworth, A. (2017). PARP Inhibitors: Synthetic Lethality in the Clinic. *Science* 355, 1152–1158, doi:10.1126/science.aam7344.
10. Agostinis, P.; Berg, K.; Cengel, K.A.; Foster, T.H.; Girotti, A.W.; et al. (2011). Photodynamic Therapy of Cancer: An Update. *CA Cancer J Clin* 61, 250–281, doi:10.3322/caac.20114.
11. Falk-Mahapatra, R.; Gollnick, S.O. (2020). Photodynamic Therapy and Immunity: An Update. *Photochem Photobiol* 96, 550–559, doi:10.1111/php.13253.
12. Moinard, M.; Augustin, J.; Carrier, M.; Da Maia, E.; Penel, A.; et al. (2022). Residual Microscopic Peritoneal Metastases after Macroscopic Complete Cytoreductive Surgery for Advanced High-Grade Serous Ovarian Carcinoma: A Target for Folate Receptor Targeted Photodynamic Therapy? *Pharmaceuticals (Basel)* 15, 1034, doi:10.3390/ph15081034.
13. Delaney, T.F.; Sindelar, W.F.; Tochner, Z.; Smith, P.D.; Friauf, W.S.; et al. (1993). Phase I Study of Debulking Surgery and Photodynamic Therapy for Disseminated Intraperitoneal Tumors. *International Journal of Radiation Oncology*Biophysics* 25, 445–457, doi:10.1016/0360-3016(93)90066-5.
14. Hahn, S.M.; Fraker, D.L.; Mick, R.; Metz, J.; Busch, T.M.; et al. (2006). A Phase II Trial of Intraperitoneal Photodynamic Therapy for Patients with Peritoneal Carcinomatosis and Sarcomatosis. *Clin Cancer Res* 12, 2517–2525, doi:10.1158/1078-0432.CCR-05-1625.
15. Sindelar, W.F.; DeLaney, T.F.; Tochner, Z.; Thomas, G.F.; Dachoswki, L.J.; et al. (1991). Technique of Photodynamic Therapy for Disseminated Intraperitoneal Malignant Neoplasms. Phase I Study. *Arch Surg* 126, 318–324, doi:10.1001/archsurg.1991.01410270062011.
16. Baydoun, M.; Moralès, O.; Frochot, C.; Ludovic, C.; Leroux, B.; et al. (2020). Photodynamic Therapy Using a New Folate Receptor-Targeted Photosensitizer on Peritoneal Ovarian Cancer Cells Induces the Release of Extracellular Vesicles with Immunoactivating Properties. *J Clin Med* 9, doi:10.3390/jcm9041185. Baydoun,
17. M.; Boidin, L.; Leroux, B.; Vignion-Dewalle, A.-S.; Quilbe, A.; Grolez, G.P.; et al. (2023). Folate Receptor Targeted Photodynamic Therapy: A Novel Way to Stimulate Anti-Tumor Immune Response in Intraperitoneal Ovarian Cancer. *Int J Mol Sci* 24, 11288, doi:10.3390/ijms241411288.
18. Sachs, N.; Clevers, H. (2014). Organoid Cultures for the Analysis of Cancer Phenotypes. *Curr Opin Genet Dev* 24, 68–73, doi:10.1016/j.gde.2013.11.012.
19. Rizvi, I.; Nath, S.; Obaid, G.; Ruhi, M.K.; Moore, K.; et al. (2019). Combination of Visudyne and a Lipid- Anchored Liposomal Formulation of Benzoporphyrin Derivative Enhances Photodynamic Therapy Efficacy in a 3D Model for Ovarian Cancer. *Photochem Photobiol* 95, 419–429, doi:10.1111/php.13066.
20. Xu, H.; Lyu, X.; Yi, M.; Zhao, W.; Song, Y.; et al. (2018). Organoid Technology and Applications in Cancer Research. *J Hematol Oncol* 11, 116, doi:10.1186/s13045-018-0662-9.
21. Maenhoudt, N.; Defraye, C.; Boretto, M.; Jan, Z.; Heremans, R.; et al. (2020). Developing Organoids from Ovarian Cancer as Experimental and Preclinical Models. *Stem Cell Reports* 14, 717–729, doi:10.1016/j.stemcr.2020.03.004.
22. Senkowski, W.; Gall-Mas, L.; Falco, M.M.; Li, Y.; Lavikka, K.; et al. (2023). A Platform for Efficient Establishment and Drug-Response Profiling of High-Grade Serous Ovarian Cancer Organoids. *Dev Cell* 58, 1106–1121.e7, doi:10.1016/j.devcel.2023.04.012.
23. de Witte, C.J.; Espejo Valle-Inclan, J.; Hami, N.; Löhmußaar, K.; Kopper, et al. (2020). Patient-Derived Ovarian Cancer Organoids Mimic Clinical Response and Exhibit Heterogeneous Inter- and Inpatient Drug Responses. *Cell Rep* 31, 107762, doi:10.1016/j.celrep.2020.107762.
24. Thorel, L.; Morice, P.-M.; Paysant, H.; Florent, R.; Babin, G.; et al. (2023). Comparative Analysis of Response to Treatments and Molecular Features of Tumor-Derived Organoids versus Cell Lines and PDX Derived from the Same Ovarian Clear Cell Carcinoma. *J Exp Clin Cancer Res* 42, 260, doi:10.1186/s13046-023-02809-8.
25. Driehuis, E.; Spelier, S.; Beltrán Hernández, I.; de Bree, R.; M Willems, S.; et al. (2019). Patient-Derived Head and Neck Cancer Organoids Recapitulate EGFR Expression Levels of Respective Tissues and Are Responsive to EGFR-Targeted Photodynamic Therapy. *J Clin Med* 8, doi:10.3390/jcm8111880.
26. Rizvi, I.; Celli, J.P.; Evans, C.L.; Abu-Yousif, A.O.; Muzikansky, A.; et al. (2010). Synergistic Enhancement of Carboplatin Efficacy with Photodynamic Therapy in a Three-Dimensional Model for Micrometastatic Ovarian Cancer. *Cancer Res* 70, 9319–9328, doi:10.1158/0008-5472.CAN-10-1783.
27. Vernon, M.; Lambert, B.; Meryet-Figuère, M.; Brotin, E.; Weiswald, L.-B.; et al. (2020). Functional miRNA Screening Identifies Wide-Ranging Antitumor Properties of miR-3622b-5p and Reveals a New Therapeutic Combination Strategy in Ovarian Tumor Organoids. *Mol Cancer Ther* 19, 1506–1519, doi:10.1158/1535-7163.MCT-19-0510.
28. Florent, R.; Weiswald, L.-B.; Lambert, B.; Brotin, E.; Abeillard, E.; et al. (2020). Puma and Noxa Upregulation by Naftopidil Sensitizes Ovarian Cancer to the BH3-Mimetic

- ABT-737 and the MEK Inhibitor Trametinib. *Cell Death Dis* 11, 380, doi:10.1038/s41419-020-2588-8.
29. Gulia, S.; Kannan, S.; Ghosh, J.; Rath, S.; Maheshwari, A.; et al. (2022). Maintenance Therapy with a Poly(ADP-Ribose) Polymerase Inhibitor in Patients with Newly Diagnosed Advanced Epithelial Ovarian Cancer: Individual Patient Data and Trial-Level Meta-Analysis. *ESMO Open* 7, 100558, doi:10.1016/j.esmoop.2022.100558.
 30. Rose, M.; Burgess, J.T.; O'Byrne, K.; Richard, D.J.; Bolderson, E. (2020). PARP Inhibitors: Clinical Relevance, Mechanisms of Action and Tumor Resistance. *Front Cell Dev Biol* 8, 564601, doi:10.3389/fcell.2020.564601.
 31. Lei, S.; Ge, F.; Lin, M.; Wang, X.; Shen, J.; et al. (2022). PARP Inhibitors Diminish DNA Damage Repair for the Enhancement of Tumor Photodynamic Therapy. *Photodiagnosis Photodyn Ther* 40, 103058, doi:10.1016/j.pdpdt.2022.103058.
 32. Tanaka, M.; Sasaki, M.; Suzuki, T.; Nishie, H.; Kataoka, H. (2021). Combination of Talaporfin Photodynamic Therapy and Poly (ADP- Ribose) Polymerase (PARP) Inhibitor in Gastric Cancer. *Biochem Biophys Res Commun* 539, 1–7, doi:10.1016/j.bbrc.2020.12.073.
 33. Sorrin, A.; Dasgupta, A.; McNaughton, K.; Arnau Del Valle, C.; Zhou, K.; et al. (2024). Co-Packaged PARP Inhibitor and Photosensitizer for Targeted Photo-Chemotherapy of 3D Ovarian Cancer Spheroids. *Cell Biosci* 14, 20, doi:10.1186/s13578-024-01197-6.
 34. Driehuis, E.; Spelier, S.; Beltrán Hernández, I.; de Bree, R.; M Willems, S.; et al. (2019). Patient-Derived Head and Neck Cancer Organoids Recapitulate EGFR Expression Levels of Respective Tissues and Are Responsive to EGFR-Targeted Photodynamic Therapy. *J Clin Med* 8, 1880, doi:10.3390/jcm8111880.
 35. Dumont, S.; Jan, Z.; Heremans, R.; Van Gorp, T.; Vergote, I.; et al. (2019). Organoids of Epithelial Ovarian Cancer as an Emerging Preclinical in Vitro Tool: A Review. *J Ovarian Res* 12, 105, doi:10.1186/s13048-019-0577-2.
 36. Weiswald, L.-B.; Bellet, D.; Dangles-Marie, V. (2015). Spherical Cancer Models in Tumor Biology. *Neoplasia* 17, 1–15, doi:10.1016/j.neo.2014.12.004.
 37. Thorel, L.; Perréard, M.; Florent, R.; Divoux, J.; Coffy, S.; et al. (2024). Patient-Derived Tumor Organoids: A New Avenue for Preclinical Research and Precision Medicine in Oncology. *Exp Mol Med* 56, 1531–1551, doi:10.1038/s12276-024-01272-5.
 38. Chakrabarti, J.; Holokai, L.; Syu, L.; Steele, N.; Chang, J.; et al. (2018). Mouse-Derived Gastric Organoid and Immune Cell Co-Culture for the Study of the Tumor Microenvironment. *Methods Mol Biol* 1817, 157–168, doi:10.1007/978-1-4939-8600-2_16.
 39. Chan, I.S.; Ewald, A.J. (2022). Organoid Co-Culture Methods to Capture Cancer Cell-Natural Killer Cell Interactions. *Methods Mol Biol* 2463, 235–250, doi:10.1007/978-1-0716-2160-8_17.
 40. Qin, X.; Sufi, J.; Vlckova, P.; Kyriakidou, P.; Acton, S.E.; et al. (2020). Cell-Type-Specific Signaling Networks in Heterocellular Organoids. *Nat Methods* 17, 335–342, doi:10.1038/s41592-020-0737-8.
 41. Tsai, S.; McOlash, L.; Palen, K.; Johnson, B.; Duris, C.; et al. (2018). Development of Primary Human Pancreatic Cancer Organoids, Matched Stromal and Immune Cells and 3D Tumor Microenvironment Models. *BMC Cancer* 2018, 18, 335, doi:10.1186/s12885-018-4238-4.



This work is licensed under Creative Commons Attribution 4.0 License

To Submit Your Article Click Here:

[Submit Manuscript](#)

DOI:10.31579/2690-4861/604

Ready to submit your research? Choose Auctores and benefit from:

- fast, convenient online submission
- rigorous peer review by experienced research in your field
- rapid publication on acceptance
- authors retain copyrights
- unique DOI for all articles
- immediate, unrestricted online access

At Auctores, research is always in progress.

Learn more <https://auctoresonline.org/journals/international-journal-of-clinical-case-reports-and-reviews>